7 GAUSSIAN MODELS

7.1 THE GAUSSIAN APPROACH

The Gaussian plume model is the most common air pollution model. It is based on a simple formula that describes the three-dimensional concentration field generated by a point source under stationary meteorological and emission conditions. The Gaussian plume model is visualized in Figure 7–1, where, for simplicity, the plume is advected toward the positive x–axis. In a general reference system, the Gaussian plume formula is expressed by

$$c = \frac{Q}{2\pi\sigma_h\sigma_z|\bar{\mathbf{u}}|}\exp\left[-\frac{1}{2}\left(\frac{\Delta_{cw}}{\sigma_h}\right)^2\right]\cdot\exp\left[-\frac{1}{2}\left(\frac{z_s+\Delta h-z_r}{\sigma_z}\right)^2\right] \quad (7\text{–}1)$$

where $c(\mathbf{s},\mathbf{r})$ is the concentration at $\mathbf{r} = (x_r, y_r, z_r)$ due to the emissions at $\mathbf{s} = (x_s, y_s, z_s)$; Q is the emission rate; $\sigma_h(j_h, d)$ and $\sigma_z(j_z, d)$ are the standard deviations (horizontal and vertical) of the plume concentration spatial distribution (often σ_h is referred to as σ_y); j_h and j_z are the horizontal and vertical turbulence states (further discussed below); d is the downwind distance of the receptor from the source, where

$$d = [(\mathbf{r}-\mathbf{s})\cdot\bar{\mathbf{u}}]/|\bar{\mathbf{u}}| \quad (7\text{–}2)$$

$\bar{\mathbf{u}}$ is the average wind velocity vector $(\bar{u}_x, \bar{u}_y, \bar{u}_z)$ at the emission height (it is assumed that $\bar{u}_z \ll (\bar{u}_x^2+\bar{u}_y^2)^{1/2}$); Δ_{cw} is the crosswind distance between the receptor and source (i.e., between the receptor and the plume centerline), where

$$\Delta_{cw} = (|\mathbf{r}-\mathbf{s}|^2 - d^2)^{1/2} \quad (7\text{–}3)$$

and Δh is the emission plume rise, which is a function of emission parameters, meteorology and downwind distance d. Equation 7–1 is applied for $d > 0$; if $d \leq 0$, then $c = 0$.

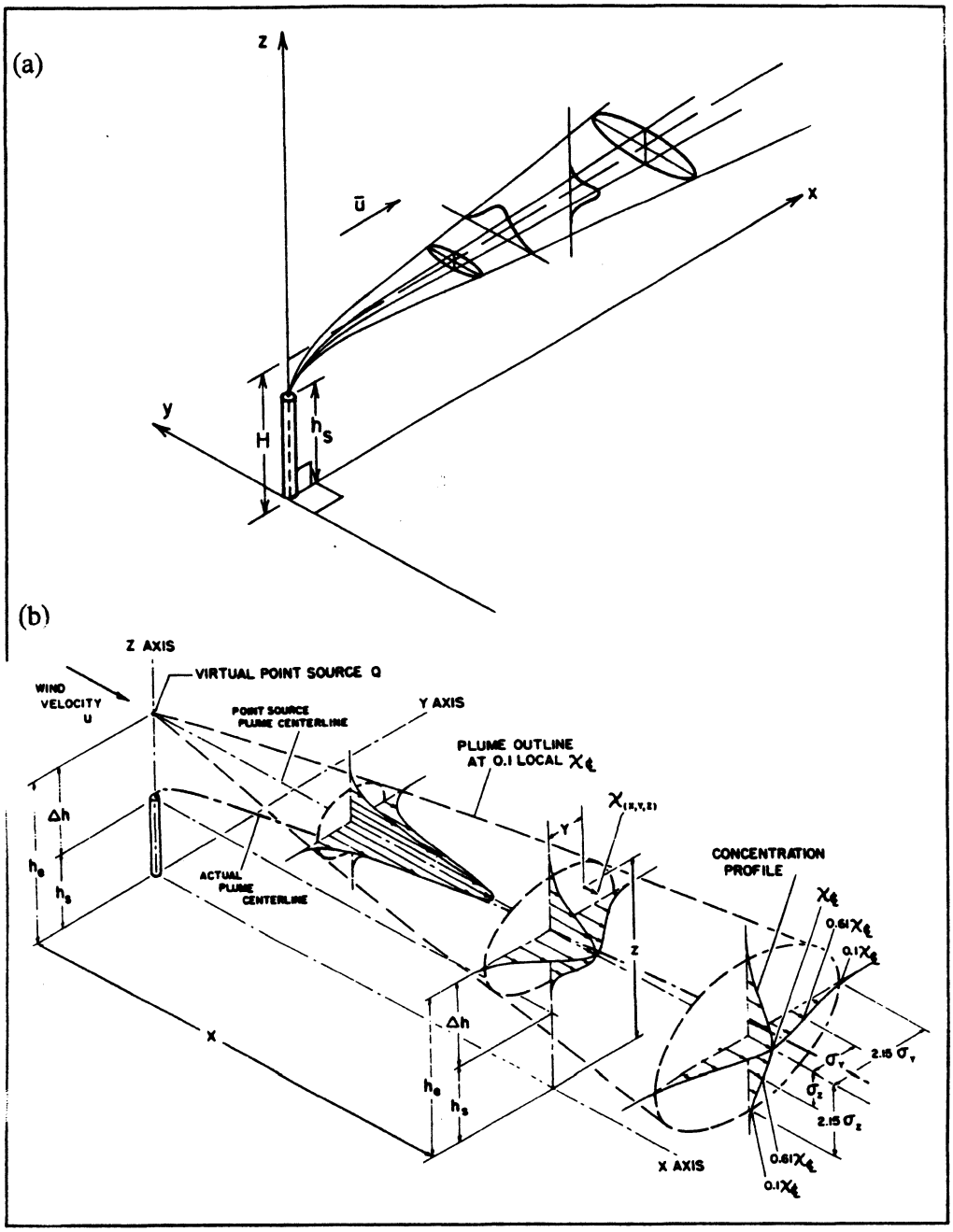

Figure 7–1. The Gaussian plume in a wind-oriented coordinate system (i.e., x along the direction of $\bar{u}$): (a) an elevated source location at (0,0,H) (from Dobbins, 1979). [Reprinted with permission from Academic Press.] (b) three-dimensional concentration profiles (from Strom; in Stern, 1976). [Reprinted with permission from Wiley–Interscience.]

As can easily be seen, Equation 7-1 refers to a stationary state (i.e., c is not a function of time), uses meteorological conditions (wind and turbulence states) that must be considered homogeneous and stationary in the modeled area (i.,e., between s and r), and cannot work in calm conditions where $|\bar{u}| \to 0$. However, the simplicity of the Gaussian approach, its relative ease of use with easily measurable meteorological parameters and, especially, the elevation of this methodology to the quantitative decision-controlling level (U.S. EPA, 1978) have stimulated research aimed at removing some of the limits of the Gaussian theory in treating the complex situations of the real world.

Equation 7-1 is generally written in the form

$$c = \frac{Q}{2\pi\,\sigma_y\,\sigma_z\,\bar{u}} \exp\left[-\frac{1}{2}\left(\frac{y_r}{\sigma_y}\right)^2\right] \exp\left[-\frac{1}{2}\left(\frac{h_e - z_r}{\sigma_z}\right)^2\right] \qquad (7\text{-}4)$$

in which $\bar{u}$ is the average horizontal wind speed, h_e is the effective emission height (i.e., $h_e = z_s + \Delta h$), and σ_y replaces σ_h. Here a wind-oriented coordinate system is also used (as in Figure 7-1). Equation 7-4 can be derived in several ways from different assumptions (see Section 7-10) and can be justified by semiempirical considerations, as Figure 7-2 illustrates, where both the instantaneous and the one-hour average concentration distributions are exemplified. It

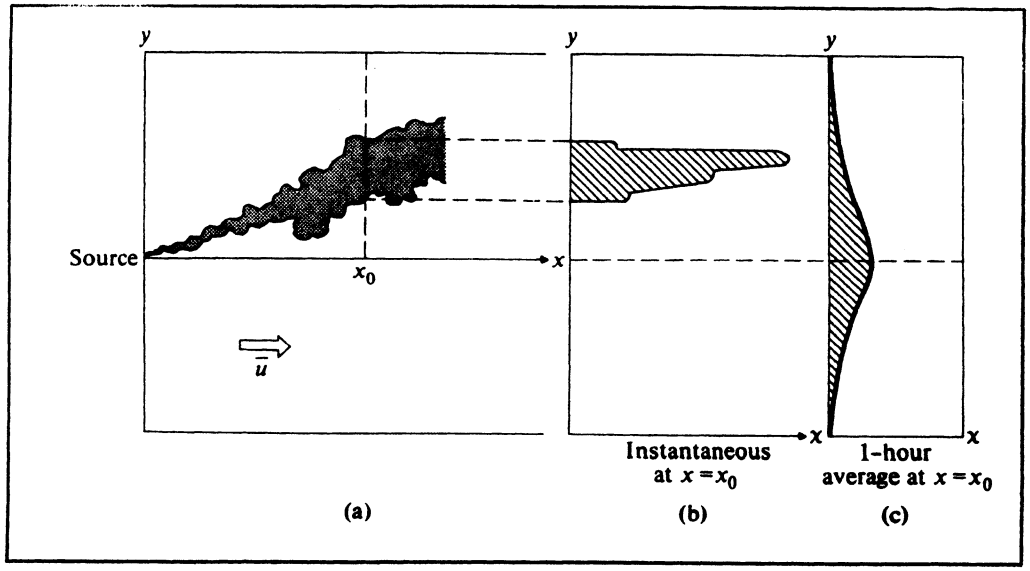

Figure 7-2. *(a) Instantaneous top view of a plume; (b) instantaneous horizontal profile of the plume concentration along a transverse direction at some distance downwind from the source; (c) one-hour average profile for the same downwind distance (from Williamson, 1973). [Reprinted with permission from Addison-Wesley.]*

can be concluded that, even though instantaneous plume concentrations are quite irregular, a sufficiently long averaging time (e.g., one hour) generates, in many cases, bell-shaped concentration distributions that can be well approximated by the Gaussian distribution in both the horizontal and (to a lesser degree) the vertical.

One area of particular emphasis has been the identification, for both simple and complex meteorological or terrain situations, of those parameters that allow Equation 7-4 to give a good estimate of the maximum ground-level concentration. Other applications have used Equation 7-4 in a "climatological" way to provide long-term concentration averages (monthly, seasonally, or annually) at the receptors (e.g., Martin, 1971; Runca et al., 1976). In these climatological applications, each concentration computed by an equation similar to Equation 7-4 is weighted by the frequency of occurrence of its corresponding meteorological condition (see Section 7.6). Other applications have even tried to remove the physical meaning of some of the parameters in Equation 7-4. For example, Melli and Runca (1979) allowed the "wind speed" $\bar{u}$ to change its value as a function of the downwind distance, to produce ground-level concentration values more like those obtained by finite-difference simulations of the same conditions.

In the past, the more complex time-varying applications of simulation modeling techniques have made extensive use of dynamic grid models (mainly, finite-difference simulations following the K-theory approach, as discussed in Chapter 6). However, a growing concern has arisen about some important limitations of such a numerical approach. Specifically, as discussed in Chapter 6, (1) the numerical treatment of the advection terms often produces an unreasonable, artificial diffusion, and (2) K-theory simulation of the growth of a plume from a point source is often fundamentally wrong in turbulent flows. Other well-known limitations are that (3) concentrations are computed as spatial averages in three-dimensional cells (which makes comparison with point measurements difficult and produces an erroneous initial dilution of plumes whose width is smaller than the cell dimensions), and (4) relating the diffusion coefficients K to standard atmospheric measurements is difficult. Also, a numerically correct application of the K-theory requires the grid size to be much less than the plume size, a condition that is difficult to satisfy near the source.

To overcome some of these limitations, modelers have attempted to extend the applicability of the Gaussian method to treat nonstationary, nonhomogeneous conditions. In particular, the segmented plume approach (Chan and Tombach, 1978; Chan, 1979) and the puff approach (Lamb, 1969; Roberts

et al., 1970) were defined to handle pseudosteady-state conditions. Both methods break up the plume into a series of independent elements (segments or puffs) that evolve in time as a function of temporally and spatially varying meteorological conditions. Sections 7.7 through 7.9 will discuss these extensions of the Gaussian approach.

7.2 THE CALCULATION OF σ_y AND σ_z

Concentrations computed by Equation 7–4 depend strongly upon a correct calculation of σ_y and σ_z, which is a major challenge for all Gaussian model applications. We present, in the two subsections below, two general methods for computing σ_y and σ_z. The first method — the preferred one — is based on the calculation of nondimensional functions and makes direct use of turbulence intensity measurements, when available. The second method relies on semiempirical calculations in which the atmosphere is classified into "stability" classes and different σ functions are derived for each class.

7.2.1 The Nondimensional S_y and S_z Functions for the Gaussian Model

Pasquill (1971) suggested the following relationships for plume sigmas, which are consistent with Taylor's statistical theory of diffusion:

$$\sigma_y = \sigma_v \, t \, S_y(t/T_L) \tag{7–5}$$

$$\sigma_z = \sigma_w \, t \, S_z(t/T_L) \tag{7–6}$$

where σ_v and σ_w are the standard deviations of the crosswind and vertical wind vector components (which can be either measured or estimated by the formulae provided in Chapter 3), and S_y and S_z are universal functions of the diffusion (or travel) time t and the Lagrangian time scale T_L. One of the major objectives of current research on Gaussian models is the computation of its nondimensional functions S_y and S_z. In this formulation, it is important to point out that σ_v must include the contribution of the wind direction meandering component.

Draxler (1976) rewrote the above equations as

$$\sigma_y = \sigma_\theta \, x \, S_y(t/T_i) \tag{7–7}$$

$$\sigma_z = \sigma_\phi \, x \, S_z(t/T_i) \tag{7–8}$$

where σ_θ and σ_ϕ are the standard deviations of wind vector azimuth and elevation angles (in radians), x is the downwind distance, and T_i is a normalization factor, proportional to T_L (i.e., $T_L = T_i/1.64$, where T_i is the time required for S_y or S_z to become equal to 0.5; S_y and S_z are always equal to 1 for $t = 0$). Note that $\sigma_\theta = \arctan(\sigma_v/\bar{u})$ and $\sigma_\phi = \arctan(\sigma_w/\bar{u})$, where, for small angles, $\sigma_\theta \simeq \sigma_v/\bar{u}$ and $\sigma_\phi \simeq \sigma_w/\bar{u}$.

Draxler (1976) also analyzed available dispersion data, giving a preliminary evaluation of the specific forms of S_y and S_z and determining T_i. Pasquill (1976) tabulated S_y as a universal function of x only. These tabulated values were then reformulated by Irwin (1979) as

$$S_y(x) = (1 + 0.0308\, x^{0.4548})^{-1} \tag{7-9}$$

for $x \leq 10^4$ m, and

$$S_y(x) = 0.333(10,000/x)^{0.5} \tag{7-10}$$

for $x > 10^4$ m.

The above formulation of S_y is currently accepted as the best way for determining σ_y and has been recommended by the American Meteorological Society Workshop on Stability Classification Schemes and Sigma Curves (Hanna et al., 1977). Phillips and Panofsky (1982), however, suggest a different S_y formulation, which provides a better fit of experimental data for small x and is consistent with inertial-subrange theory, namely

$$S_y = 0.617\left[\frac{T_i}{t} - \frac{(T_i/t)^2}{5.25}\ln\left(1 + 5.25\,\frac{t}{T_i}\right)\right]^{1/2} \tag{7-11}$$

Much investigation is still required to fully evaluate the validity of the above S_y formulations. In particular, the dependence of S_y only upon x is certainly questionable. Incidentally, Lagrangian particle dispersion numerical experiments (e.g., Zannetti and Al-Madani, 1983a,b) have confirmed a behavior of σ_y in agreement with the statistical theory of diffusion and showed a variability of σ_y values, from the same σ_θ input, associated with changes in the autocorrelation structure of the wind direction (that is, a higher time correlation in the wind direction θ is causing, as expected, larger σ_y, even though σ_θ is the same).

The evaluation of S_z is still quite uncertain. Irwin (1979) provided a preliminary universal function S_z and recommended its interim use until more field

data permit the evaluation of a more accurate scheme. In unstable conditions, his S_z function depends upon the depth of the mixing layer h, the diffusion time t, the effective release height h_e, the surface friction velocity u_* and the Monin–Obukov length scale L. Also, Draxler (1976) derived, under neutral and stable conditions,

$$S_z = [1 + 0.9(t/T_o)^{1/2}]^{-1} \tag{7-12}$$

for $z < 50$ m, and

$$S_z = [1 + 0.945(t/T_o)^{0.8}]^{-1} \tag{7-13}$$

for $z \geq 50$ m, in which the characteristic time T_o is $\simeq 50$ s.

Additional considerations on the calculation of S_y and S_z for travel distances less than 10 km in the different layers of the PBL (see Figure 3–8) can be found in Gryning et al. (1987), who, however, propose non-Gaussian vertical concentration profiles in most cases.

It must be pointed out that only the availability of *validated* S_y and S_z functions allows a proper application of Gaussian modeling techniques in a way that makes full use of available meteorological measurements of the standard deviations of the wind vector components. In fact, the simple use of semi-empirical plume sigmas (as discussed below) requires only the evaluation of the stability class (a discrete number) and cannot make use of the exact information on wind fluctuation intensities, when available.

7.2.2 Semiempirical σ Calculations

Several schemes that allow the computation of σ_y and σ_z from the atmospheric stability class and the downwind distance are available. The stability class can be computed using the Pasquill or Turner methods (see Tables 3–2 and 3–3) or from measurements of either σ_θ or σ_w or the vertical temperature gradient $\Delta T/\Delta z$, as Tables 7–1 and 7–2 illustrate. Nighttime conditions are sometimes characterized, especially with low wind speed, by large horizontal dispersion due to wind direction meandering and small vertical dispersion due to the ground-based temperature inversion. Therefore, when stability is evaluated using the standard deviation of the horizontal wind direction fluctuations (see Table 7–2), this stability must be corrected according to Table 7–3 in order to characterize vertical diffusion at nighttime.

Full three-dimensional tracer experiments have shown that horizontal and vertical diffusion rates are often related to different stability categorizations and,

Table 7-1.—Classification of atmospheric stability (data from DeMarrais, 1978; Best et al., 1986; and Hanna, 1989).

Stability classification	Pasquill categories	σ_θ (*) (degrees)	ΔT temperature change with height (°C 10^{-2} m^{-1})	R_i gradient Richardson number at 2 m	$\sigma_w/\bar{u}$
Extremely unstable	A	25.0	< -1.9	-0.9	> 0.15
Moderately unstable	B	20.0	-1.9 to -1.7	-0.5	0.1 - 0.15
Slightly unstable	C	15.0	-1.7 to -1.5	-0.15	
Neutral	D	10.0	-1.5 to -0.5	0	0.05 - 0.1
Slightly stable	E	5.0	-0.5 to 1.5	0.4	
Moderately stable	F	2.5	1.5 to 4.0	0.8	0.0 - 0.05
Extremely unstable	G	1.7	> 4.0		

(*) Standard deviation of horizontal wind direction fluctuation over a period of 15 minutes to 1 hour. The values shown are averages for each stability classification.

Table 7-2. Classification of atmospheric stability[1] (from U.S. EPA, 1986, adapted from Irwin, 1980).

Pasquill stability categories	Standard deviation of the horizontal wind direction fluctuations [2] (degrees)	Standard Deviation of the vertical wind direction fluctuations [2] (degrees)
A	Greater than 22.5°	Greater than 11.5°
B	17.5 to 22.5°	10.0° to 11.5°
C	12.5° to 17.5°	7.8° to 10.0°
D	7.5° to 12.5°	5.0° to 7.8°
E	3.8° to 7.5°	2.4° to 5.0°
F	Less than 3.8°	Less than 2.4°

[1] These criteria are appropriate for steady-state conditions, a measurement height of 10 m, for level terrain, and an aerodynamic surface roughness length of 15 cm. Care should be taken that the wind sensor is responsive enough for use in measuring wind direction fluctuation.

[2] A surface roughness factor of $(z_o/15\ \text{cm})^{0.2}$, where z_o is the average surface roughness in centimeters within a radius of 1-3 km of the source, may be applied to the table values. This factor, while theoretically sound, has not been subjected to rigorous testing and may not improve the estimates in all circumstances.

Table 7–3. Nighttime(*) (vertical) Pasquill stability category based on σ_θ ; i.e., the standard deviation of the horizontal wind direction fluctuations, in degrees (from U.S. EPA, 1986, adapted from Irwin, 1980).

If the σ_θ stability category is	And the wind speed at 10 m is ($m\ s^{-1}$)	Then the Pasquill stability category is
A	< 2.9	F
	2.9 to 3.6	E
	≥ 3.6	D
B	< 2.4	F
	2.4 to 3.0	E
	≥ 3.0	D
C	< 2.4	E
	≥ 2.4	D
D	wind speed not considered	D
E	wind speed not considered	E
F	wind speed not considered	F

(*) Nighttime is considered to be from one hour before sunset to one hour after sunrise.

therefore, a "split-sigma" approach should generally be adopted, in which σ_y and σ_z dynamics are evaluated as functions of "horizontal" and "vertical" stability classes, respectively. Results indicate that σ_θ measurements provide a good estimate of the "horizontal" stability, while vertical temperature gradient data seem appropriate for identifying the "vertical" stability class.

After the computation of the stability class, σ_y and σ_z can be computed at a certain downwind distance x by choosing one of the several available formulae:

1. Pasquill–Gifford sigmas (Gifford, 1961) graphically presented by Turner (1970) and, in an analytical form, by Green et al. (1980), as

$$\sigma_y(x) = \frac{k_1\, x}{[1 + (x/k_2)]^{k_3}} \tag{7–14}$$

$$\sigma_z(x) = \frac{k_4\, x}{[1 + (x/k_2)]^{k_5}} \tag{7–15}$$

where the constants k_1, k_2, k_3, k_4, k_5 are given in Table 7–4.

Table 7–4. Values of the constants in the Equations 7–14 and 7–15.

Stability class	k_1	k_2	k_3	k_4	k_5
A	0.250	927	0.189	0.1020	−1.918
B	0.202	370	0.162	0.0962	−0.101
C	0.134	283	0.134	0.0722	0.102
D	0.0787	707	0.135	0.0475	0.465
E	0.0566	1,070	0.137	0.0335	0.624
F	0.0370	1,170	0.134	0.0220	0.700

The above σ_y, σ_z values were derived (Gifford, 1976) primarily from a diffusion experiment in flat terrain ($z_o \simeq 0.03$ m) in which a nonbuoyant tracer gas was released near the surface and measured (three-minute averages) downwind up to a distance of 800 m from the source. Pasquill–Gifford sigmas are the most used formulation for U.S. EPA regulatory modeling applications.

2. Brookhaven sigmas (Smith, 1968), in which a power law function is assumed for both σ_y and σ_z; i.e.,

$$\sigma = a\,x^b \tag{7–16}$$

Table 7–5 gives the coefficients a and b for each "gustiness" category. Table 7–6 illustrates the relation between the "gustiness" categories and the Pasquill classes. The Brookhaven scheme was derived from elevated releases (108 m) over a rough surface ($z_o \simeq$ 1 m), with concentrations measured up to a few kilometers downwind.

3. Briggs sigmas (Briggs, 1973), in urban and rural versions, provide an interpolation scheme that agrees with Pasquill–Gifford in the downwind range from 100 m to 10 km, except that σ_z values for A and B stability approximate the B_2 and B_1 Brookhaven curves. Table 7–7 gives the Briggs sigmas. The urban Briggs sigmas are also called McElroy–Pooler sigmas, and were derived from several

Table 7–5. Coefficients a and b for Equation 7–16.

Gustiness category	σ_y		σ_z	
	a	*b*	*a*	*b*
B_2	0.40	0.91	0.41	0.91
B_1	0.36	0.86	0.33	0.86
C	0.32	0.78	0.22	0.78
D	0.31	0.71	0.06	0.71

Table 7–6. Relation between the "gustiness" category and the Pasquill class (from Gifford, 1976).

Pasquill class	Gustiness category
A	B_2 (very unstable)
B	B_1 (unstable)
C	B_1 (unstable
D	C (neutral)
E	C/D (neutral/stable)
F	D (stable)

urban dispersion experiments with low-level tracers (McElroy and Pooler, 1968). The U.S. EPA recommends these sigma values as the ones most appropriate for dispersion simulations in urban areas (U.S. EPA, 1984).

Table 7–7. The Briggs (1973) sigma functions for (a) urban and (b) rural conditions (from Panofsky and Dutton, 1984). [Reprinted with permission from Wiley–Interscience.]

(a) Urban Dispersion Parameters (for distances between 100 and 10,000 m)

Pasquill stability	σ_y (m)	σ_z (m)
A–B	$0.32\,x\,(1 + 0.0004\,x)^{-0.5}$	$0.24\,x\,(1 + 0.001\,x)^{0.5}$
C	$0.22\,x\,(1 + 0.0004\,x)^{-0.5}$	$0.20\,x$
D	$0.16\,x\,(1 + 0.0004\,x)^{-0.5}$	$0.14\,x\,(1 + 0.0003\,x)^{-0.5}$
E–F	$0.11\,x\,(1 + 0.0004\,x)^{-0.5}$	$0.08\,x\,(1 + 0.00015\,x)^{-0.5}$

(b) Rural Dispersion Parameters (for distances between 100 and 10,000 m)

Pasquill stability	σ_y (m)	σ_z (m)
A	$0.22\,x\,(1 + 0.0001\,x)^{-0.5}$	$0.20\,x$
B	$0.16\,x\,(1 + 0.0001\,x)^{-0.5}$	$0.12\,x$
C	$0.11\,x\,(1 + 0.0001\,x)^{-0.5}$	$0.08\,x\,(1 + 0.0002\,x)^{-0.5}$
D	$0.08\,x\,(1 + 0.0001\,x)^{-0.5}$	$0.06\,x\,(1 + 0.0015\,x)^{-0.5}$
E	$0.06\,x\,(1 + 0.0001\,x)^{-0.5}$	$0.03\,x\,(1 + 0.0003\,x)^{-1}$
F	$0.04\,x\,(1 + 0.0001\,x)^{-0.5}$	$0.016\,x\,(1 + 0.0003\,x)^{-1}$

Several additional formulations and parameterizations of σ_y and σ_z are available in the literature. See, for example, Briggs (1985) for a review of diffusion parameterizations for the convective (i.e., unstable) PBL.

7.3 REFLECTION TERMS

The basic Gaussian formula is often used with the assumption of total or partial concentration reflection at the surface (see Figure 7–3). Therefore, the last term in Equation 7–4 becomes

$$S(z_r) = \exp\left[-\frac{1}{2}\left(\frac{h_e - z_r}{\sigma_z}\right)^2\right] + r_g \exp\left[-\frac{1}{2}\left(\frac{h_e + z_r}{\sigma_z}\right)^2\right] \quad (7\text{–}17)$$

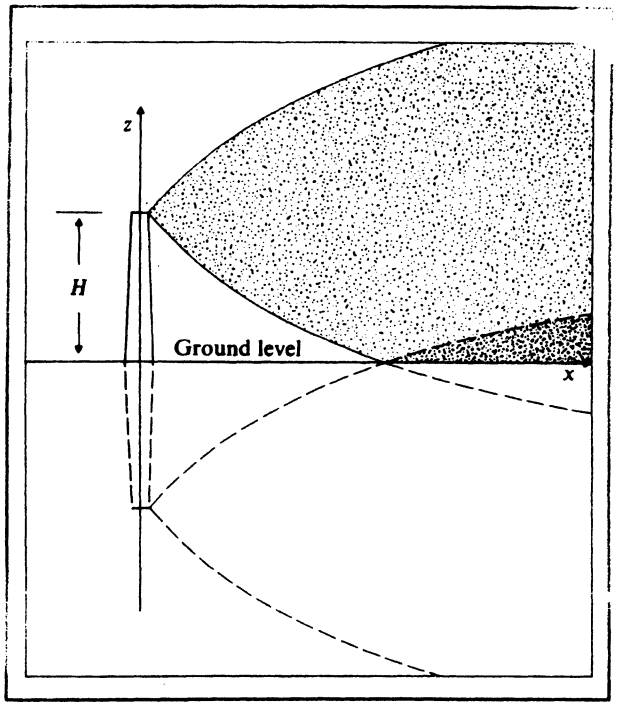

Figure 7–3. Example of ground reflection simulated by the image method; i.e., a vertical source below the ground (from Williamson, 1973). [Reprinted with permission from Addison–Wesley.]

where r_g is the ground reflection coefficient ($r_g = 1$, i.e., total reflection, is generally assumed). For receptors at the ground ($z_r = 0$) with $r_g = 1$, Equation 7–17 becomes

$$S(0) = 2 \exp\left[-\frac{1}{2}\left(\frac{h_e}{\sigma_z}\right)^2\right] \quad (7\text{–}18)$$

which, for ground-level nonbuoyant sources (i.e., $h_e = 0$), gives

$$S(0) = 2 \quad (7\text{–}19)$$

If the plume is emitted within the PBL, it can also be reflected from the top z_i of the PBL, giving

$$S(z_r) = \exp\left[-\frac{1}{2}\left(\frac{h_e - z_r}{\sigma_z}\right)^2\right] + r_g \exp\left[-\frac{1}{2}\left(\frac{h_e + z_r}{\sigma_z}\right)^2\right] + r_i \exp\left[-\frac{1}{2}\left(\frac{2z_i - h_e - z_r}{\sigma_z}\right)^2\right] \tag{7-20}$$

where r_i is the reflection coefficient at z_i ($r_i = 1$, i.e., total reflection, is generally assumed). However, the presence of a second reflecting barrier causes multiple reflections and, therefore, instead of Equation 7–20, it is better to use, for $r_g = r_i = 1$,

$$S(z_r) = \sum_{j=0,\,\pm 1,\,\pm 2,\ldots} \left\{\exp\left[-\frac{1}{2}\left(\frac{z_r + 2\,j\,z_i - h_e}{\sigma_z}\right)^2\right] + \exp\left[-\frac{1}{2}\left(\frac{z_r + 2\,j\,z_i + h_e}{\sigma_z}\right)^2\right]\right\} \tag{7-21}$$

Unfortunately, in some cases, Equation 7–21 converges slowly. To avoid excessive computations, Yamartino (1977) proposed an efficient method for approximating Equation 7–21, in which:

- for $\sigma_z/z_i \leq 0.63$, Equation 7–21 is truncated at $j = 0, \pm 1$
- for $0.63 < \sigma_z/z_i \leq 1.08$, Equation 7–21 is approximated by

$$S(z_r) = \frac{\sqrt{2\,\pi}\,\sigma_z}{z_i}(1 - \beta^2)\,[1 + \beta^2 + 2\,\beta\,\cos(\pi\,z_r/z_i)\,\cos(\pi\,h_e/z_i)] \tag{7-22}$$

where

$$\beta = \exp\left[-\frac{1}{2}\left(\frac{\pi\,\sigma_z}{z_i}\right)^2\right] \tag{7-23}$$

and, for $\sigma_z/z_i > 1.08$, Equation 7–22 is used with $\beta = 0$, giving

$$S(z_r) = \frac{\sqrt{2\pi}\sigma_z}{z_i} \tag{7-24}$$

which, substituted into Equation 7–4, gives the "trapping" equation

$$c = \frac{Q}{\sqrt{2\pi}\sigma_y \bar{u} z_i} \exp\left[-\frac{1}{2}\left(\frac{y_r}{\sigma_y}\right)^2\right] \tag{7-25}$$

Equation 7–25 shows a uniform vertical mixing (between $z = 0$ and $z = z_i$) of the plume, whose concentrations no longer depend upon z.

The above scheme approximates Equation 7–21 with an error < 1.3 percent and is, therefore, quite satisfactory in all applications.

7.4 DEPOSITION/DECAY TERMS

Dry deposition, wet deposition and chemical transformation phenomena are usually taken into account in the Gaussian model by multiplying Equation 7–4 by exponential terms such as

$$\exp\ [-t/T] \tag{7-26}$$

where t is the travel time

$$t = x/\bar{u} \tag{7-27}$$

and T is the corresponding time scale. The relation between the percentage of mass reduction per hour (%/h) and the time scale T in Equation 7–26 is

$$\%/h = 100\ [1 - \exp(-3,600/T)] \tag{7-28a}$$

and, for large T,

$$\%/h \simeq 360,000/T \tag{7-28b}$$

More discussion of atmospheric deposition phenomena is presented in Chapter 10.

7.4.1 Dry Deposition

The time scale of dry deposition, T_d, can be expressed as a function of the deposition velocity V_d (see Equation 6–10), as follows

$$\frac{1}{T_d} = V_d/\Delta_p \tag{7-29}$$

where Δ_p is the vertical thickness of the plume, say

$$\Delta_p \simeq 4\,\sigma_z \tag{7-30}$$

Since dry deposition phenomena occur only after the plume interacts with terrain features, it is often convenient to apply Equation 7–26 only beyond a critical downwind distance x_d, defined as the distance at which $2\,\sigma_z$ is equal to the height of the plume above the ground; i.e.,

$$2\,\sigma_z(x_d) = h_e \tag{7-31}$$

which can be rewritten as

$$x_d = \sigma_z^{-1}(h_e/2) \tag{7-32}$$

where $\sigma_z^{-1}(...)$ is the inverse function of $\sigma_z(x)$.

7.4.2 Wet Deposition

The time scale of the wet deposition, T_w, can be expressed (Draxler and Heffter, 1981) as

$$T_w = \frac{3.6 \cdot 10^6\, P_L}{S_r\, P_R} \tag{7-33}$$

where P_L is the thickness of the precipitation layer (an average climatological value of P_L is 4,000 m), S_r is the scavenging ratio of the pollutant (a typical value for SO_2 is $S_r = 4.2 \cdot 10^5$), and P_R is the precipitation rate in mm/h.

7.4.3 Chemical Transformation

The time scale of the chemical transformation, T_c, is mainly a function of the reactivity of the pollutant. A typical value for SO_2 is T_c = 100,800 s (i.e., 28 hours).

7.5 SPECIAL CASES

Several modifications of the Gaussian equation that have been proposed for simulating special dispersion conditions are discussed in this section.

7.5.1 Line, Area, and Volume Sources

Equation 7-1 or 7-4 can be spatially integrated to simulate the effects of line, area, and volume sources. Analytical integration is often impossible or requires simplifications (especially in the forms of the σ_y and σ_z functions). Therefore, numerical integration is often used for these spatial integrations. Many Gaussian models (see Chapter 14) contain accurate routines for the treatment of line, area, and volume sources.

In several cases, the virtual point source method provides a simple, but satisfactory, treatment of line, area and volume sources, without integration. Using this method, the actual nonpoint source is simulated by an appropriate upwind virtual point source S', as Figure 7-4 illustrates.

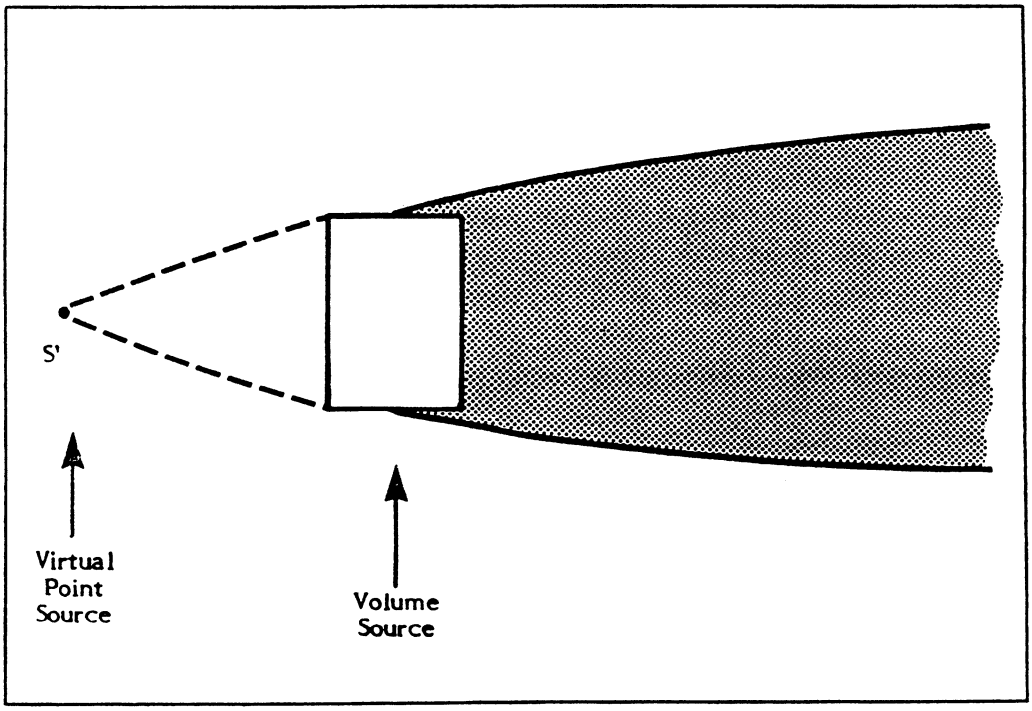

Figure 7-4. The virtual source approach for simulating line, area, and volume sources.

7.5.2 Fumigation

Turner (1970) proposed the following formula to simulate the maximum morning fumigation effects of an elevated plume previously emitted into the stable layer:

$$c(x, 0, z) = \frac{Q}{\sqrt{2\pi}\ \sigma_{yF}\ H_i\ \bar{u}} \tag{7-34}$$

where

$$H_e = h_e + 2\ \sigma_{zs} \tag{7-35}$$

$$\sigma_{yF} \simeq \sigma_{ys} + (h_e/8) \tag{7-36}$$

Equation 7–34 is derived by assuming that the stable plume, characterized by σ_{ys} and σ_{zs}, is suddenly fumigated to the ground. During this fumigation, the plume becomes homogeneously mixed in the vertical, between $z = 0$ and $z = h_e + 2\ \sigma_{zs}$, and expands horizontally following a 15° fumigation trajectory (from H_e to the ground), which causes an increase of σ_y from σ_{ys} to σ_{yF}.

7.5.3 Concentration in the Wake of Building

Several algorithms have been proposed for computing plume downwash effects, which Figure 7–5 outlines. In particular, downwash algorithms have been incorporated into two Gaussian computer codes (see Chapter 14): the Industrial Source Complex Model (ISC; Bowers et al., 1979) and the Buoyant Line and Point (BLP) Source Dispersion Model (Schulman and Scire, 1980). The ISC model was further modified (Schulman and Hanna, 1986) to account for improved understanding of plume rise and downwash around buildings.

A simple estimate of the extra diffusion induced by the buildings can be obtained by increasing the plume sigmas in the following way

$$\sigma_{yw} = (\sigma_y^2 + const\ A/\pi)^{1/2} \tag{7-37}$$

$$\sigma_{zw} = (\sigma_z^2 + const\ A/\pi)^{1/2} \tag{7-38}$$

where σ_y and σ_z are the plume sigmas without the building effects; σ_{yw} and σ_{zw} incorporate the building effects; and A is the area of the building projected onto a vertical plane normal to wind direction.

More discussion of this topic is found in Section 11.3.

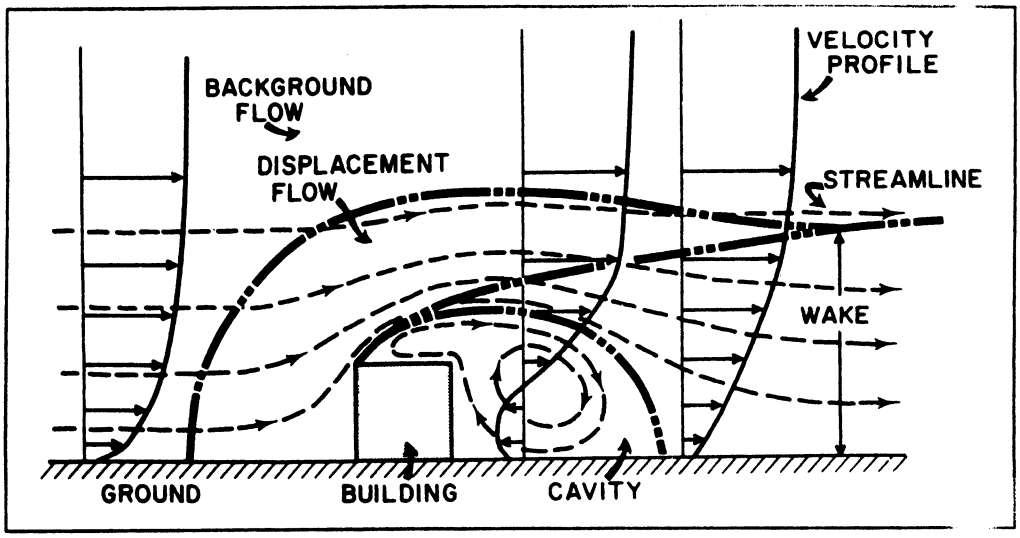

Figure 7–5. Mean flow around a cubical building. The presence of a bluff structure in otherwise open terrain will produce aberrations in the wind flow generally similar to those shown (from Smith, 1968). [Reprinted with permission from the American Society of Mechanical Engineers.]

7.5.4 Plume Trapping Into a Valley

Turner (1970) proposed to treat the plume trapping in a valley in a manner similar to the plume trapping between the ground and z_i ; i.e., similar to the trapping Equation 7–25, but in the horizontal instead of the vertical. With this assumption, in the case of simple uniform flow parallel to the valley axis along x, we obtain for any y,

$$c(x, y, 0) = \left(\frac{2}{\pi}\right)^{1/2} \frac{Q}{W \sigma_z \bar{u}} \exp\left[-\frac{1}{2}\left(\frac{h_e}{\sigma_z}\right)^2\right] \qquad (7\text{–}39)$$

where W is the valley width. Harvey and Hamawi (1986) presented an expanded analytical treatment of plume trapping in a valley.

7.5.5 Tilted Plume

Plumes of large particles having a freefall, i.e., gravitational (settling) velocity V_G can be simulated by the Gaussian tilted plume approach Figure 7–6 illustrates. The plume is tilted downward at an angle whose tangent is $V_G/\bar{u}$, the reflection coefficient at the ground is zero, and most of the plume material is

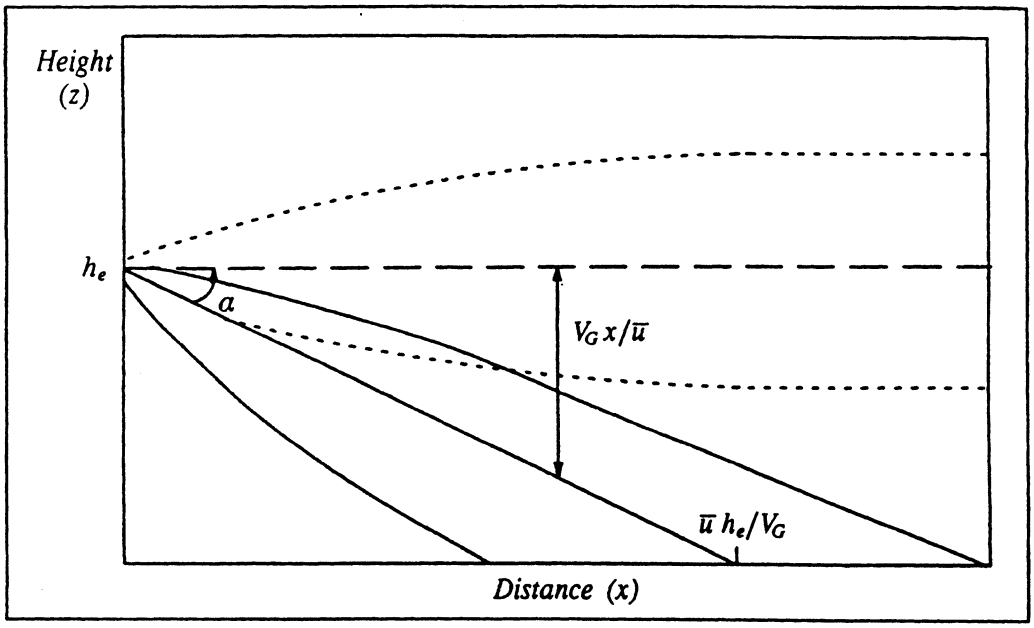

Figure 7–6. Schematic representation of tilted plume treatment of deposition of particles with settling velocity V_G. Solid lines represent the tilted plume, while dotted lines describe the plume shape with $V_G = 0$.

deposited at the ground at a distance of about $\bar{u}\, h_e/V_G$. Section 11.4 provides additional discussion.

7.5.6 Coastal Diffusion and Shoreline Fumigation

Shoreline fumigation is a particularly important problem. As Figure 7–7 illustrates, elevated plumes emitted offshore or near the shoreline initially encounter stable marine dispersion conditions. But when carried inland by the daytime breeze, they eventually penetrate the growing unstable mixing layer inland and are, therefore, fumigated to the ground.

Lyons and Cole (1973) and van Dop et al. (1979) provided the following approximate solution to the fumigation problem. If $z_i(x)$ is the mixing height,

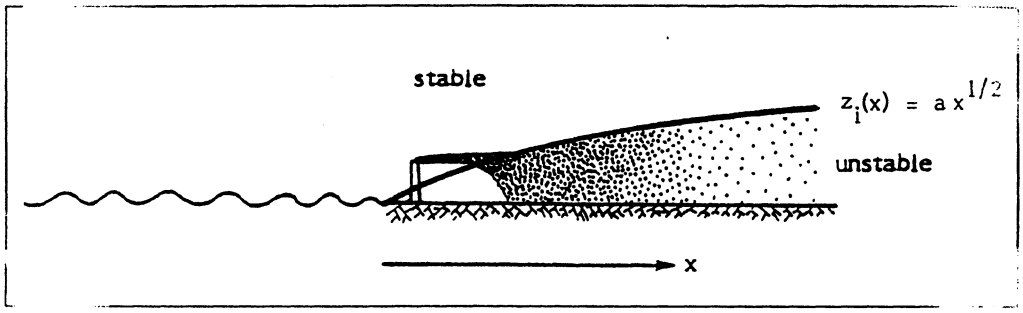

Figure 7–7. Example of plume producing uniform vertical concentration after encountering unstable layer.

expressed as a function of the distance x from the shoreline, the concentration in the fumigation region is

$$c_F(x) = \frac{1}{z_i(x)} \int_{-\infty}^{z_i(x)} c\, dz \tag{7–40}$$

where c is the concentration field generated by the standard Gaussian plume equation with stable sigmas (i.e., σ_{ys}, σ_{zs}). After some simplifying assumptions, we obtain, for small σ_{zs} and $y = 0$,

$$c_F(x) \simeq \frac{Q}{\sqrt{2\,\pi}\ \sigma_{yF}\, u\, z_i(x)} \tag{7–41}$$

where σ_{yF} has been previously defined by Equation 7–36.

A Gaussian code, developed for the U.S. Department of the Interior, simulates the overwater transport and diffusion of pollutants emitted by offshore sources, such as oil platforms. This model (offshore and coastal dispersion, OCD; Hanna et al., 1984) is becoming the official U.S. EPA regulatory tool for these applications.

Section 11.2 presents additional discussion of coastal diffusion phenomena.

7.5.7 Complex Terrain

A few Gaussian computer codes are available for complex terrain simulations. The most recent ones are the rough terrain dispersion model (RTDM; ERT,

1984) and the complex terrain dispersion model (CTDM; Strimaitis et al., 1986), both developed for the U.S. EPA. They incorporate the results of intensive tracer experiment studies in complex terrain.

One of the most important issues in complex terrain modeling by Gaussian formulae is the estimate of the plume centerline height when approaching the terrain height. Three simple assumptions are illustrated in Figure 7–8. Recent, more refined, techniques are presented in Section 11.1.

7.6 THE CLIMATOLOGICAL MODEL

The Gaussian plume equation is often used to simulate the time-varying concentration field by assuming a series of steady-state conditions. In other words, if the hourly emission and meteorological input is known, a steady-state equation (such as Equation 7–4) can be used repeatedly with the assumption that each hour can be represented by a stationary concentration field.

Several air quality applications require the computation of long-term (e.g., annual) concentration averages, thus requiring a large number of hourly

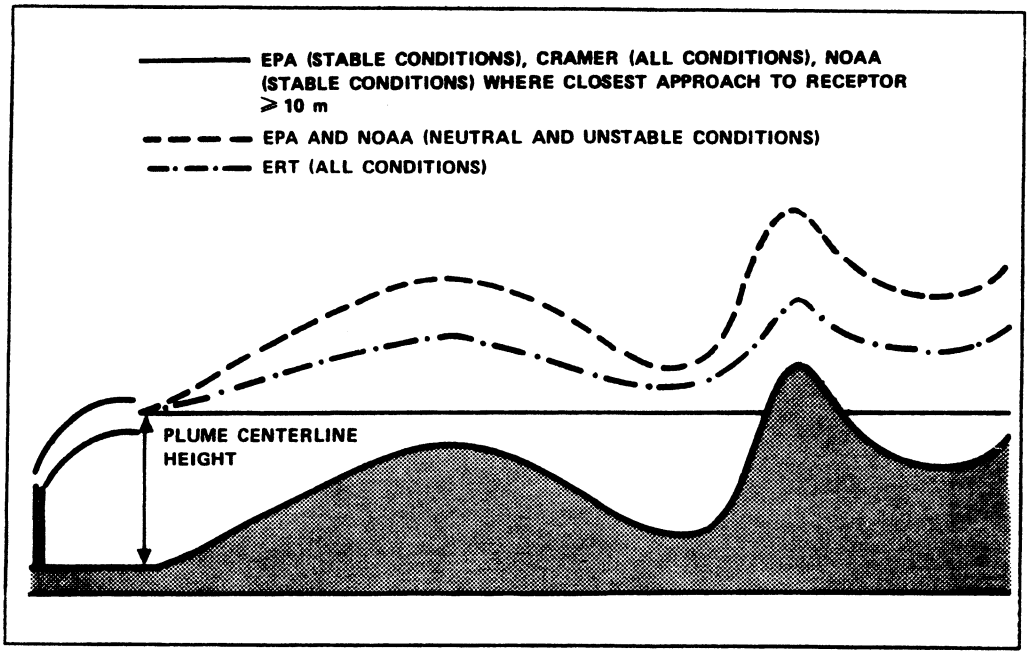

Figure 7–8. Simple assumptions for simulating plume centerline trajectory in complex terrain (from Fabrick et al., 1977). More advanced assumptions are discussed in Section 11.1.

computations (e.g., 8,760 hourly computations for each source–receptor contribution are required to estimate the annual average). Since meteorological and emission conditions are often the same at several different times, many of these hourly computations will provide the same concentration field output. The climatological model takes advantage of this repetition to compute long–term concentration averages without performing an expensive hour–by–hour simulation.

The procedure used is the following. Let us assume that a source can operate in N_i different emission conditions and that the meteorology can be described by N_j meteorological classes. Then the general climatological model equation becomes

$$\bar{c} = \sum_{i=1}^{N_i} \sum_{j=1}^{N_j} f_{ij} Q_i \psi_{ij} / \left(\sum_{i=1}^{N_i} \sum_{j=1}^{N_j} f_{ij} \right) \qquad (7\text{–}42)$$

where $\bar{c}$ is the average concentration in the receptor **r** due to the source in **s** during the period under examination; f_{ij} is the joint frequency of occurrence, during the same period, of the i–th emission condition and the j–th meteorological condition; Q_i is the pollutant emission rate during the i–th emission condition; and $Q_i \psi_{ij}$ is the steady–state equation (e.g., the Gaussian plume equation), which gives the concentration in **r** due to the emission in **s** with the i–th emission and the j–th meteorological scenarios (ψ_{ij} is referred to as the "kernel" of the concentration computation formula). If N_i x N_j is much smaller than the number of hours of the long–term period under investigation, Equation 7–42 is computationally faster than the hour–by–hour simulation and, for most practical cases, almost as accurate. Note that the term ψ_{ij} can be precomputed for all i and j, thus allowing easy recalculations with different emissions Q_i and/or different meteorology f_{ij}.

The climatological model is generally applied with the following further assumptions:

1. The Gaussian plume equation (Equation 7–4) is used for computing the kernel ψ_{ij}.

2. Q is constant (or depends only upon the meteorological condition j).

3. The meteorological condition j is given by the combination of a wind direction class j_1, a wind speed class j_2, and a stability class j_3 [i.e., f_{ij} becomes $f(j_1, j_2, j_3)$].

4. Because of the high frequency of occurrence of wind blowing in each wind direction sector, a uniform crosswind horizontal concentration distribution is assumed within each downwind sector.

5. Receptors are at ground level.

With the above assumptions, Equation 7–42 becomes

$$\bar{c} = \sum_{j_1\, j_2\, j_3} f(j_1,j_2,j_3)\, Q(j_1,j_2,j_3)\, \psi(j_1,j_2,j_3) \Big/ \left(\sum_{j_1\, j_2\, j_3} f(j_1,j_2,j_3) \right) \qquad (7\text{–}43)$$

where $\psi(j_1, j_2, j_3)$ is the uniform crosswind horizontal Gaussian kernel,

$$\psi(j_1,j_2,j_3) = \left(\frac{2}{\pi}\right)^{1/2} \frac{N_{wd}/(2\,\pi\,\Delta_d)}{\sigma_z\,\bar{u}} \exp\left[-\frac{1}{2}\left(\frac{z_s + \Delta h}{\sigma_z}\right)^2\right] \qquad (7\text{–}44)$$

Here N_{wd} is the number of wind direction sectors (i.e., $j_1 = 1, 2, \ldots, N_{wd}$; generally $N_{wd} = 16$); $\Delta_d(\mathbf{s},\mathbf{r},j_1)$ is the horizontal downwind distance between the source and the receptor; $\sigma_z(\Delta_d, j_3)$ is the vertical plume sigma; $\Delta h(j_2, j_3)$ is the plume rise; $\bar{u}(j_2)$ is the wind speed; and z_s is the source height. Equation 7–44 can be precomputed for each j_1, j_2, and j_3, thus providing a fast computational algorithm for $\bar{c}$. Clearly, Equation 7–44 must be applied only when the receptor **r** is downwind of the source **s** for the wind direction class j_2 (where downwind, in this case, means within a sector of $2\pi/N_{wd}$ angle in the horizontal); otherwise, ψ is equal to zero.

If the plume is uniformly mixed in the mixing layer, Equation 7–44 is further simplified as

$$\psi(j_1,j_2,j_3) = \frac{N_{wd}/(2\,\pi\,\Delta_d)}{z_i\,\bar{u}} \qquad (7\text{–}45)$$

where z_i is the mixing height.

Several authors (e.g., Martin, 1971; Calder, 1971; Runca et al., 1976) have used the climatological Gaussian model successfully. These long-term simulations generally provide better results than the short-term ones, due to error cancellation effects.

7.7 THE SEGMENTED PLUME MODEL

The Gaussian steady-state formula described in Equation 7-1 or 7-4 is valid only during transport conditions (e.g., $\bar{u} \geq 1$ m/s) in fairly stationary and homogeneous situations. In order to treat time-varying transport conditions and, especially, changes in wind direction, several authors (e.g., Hales et al., 1977; Benkley and Bass, 1979; Chan et al., 1979) have developed and used segmented Gaussian plume models. In the segmented plume approach, the plume is broken up into independent elements (plume segments or sections) whose initial features and time dynamics are a function of time-varying emission conditions and the local time-varying meteorological conditions encountered by the plume elements along their motion.

The segmented plume features are illustrated in Figure 7-9, which shows a plan view (solid lines) of a segmented plume encountering a progressive change of wind direction along its trajectory. Segments are sections of a Gaussian plume. Each segment, however, generates a concentration field that is

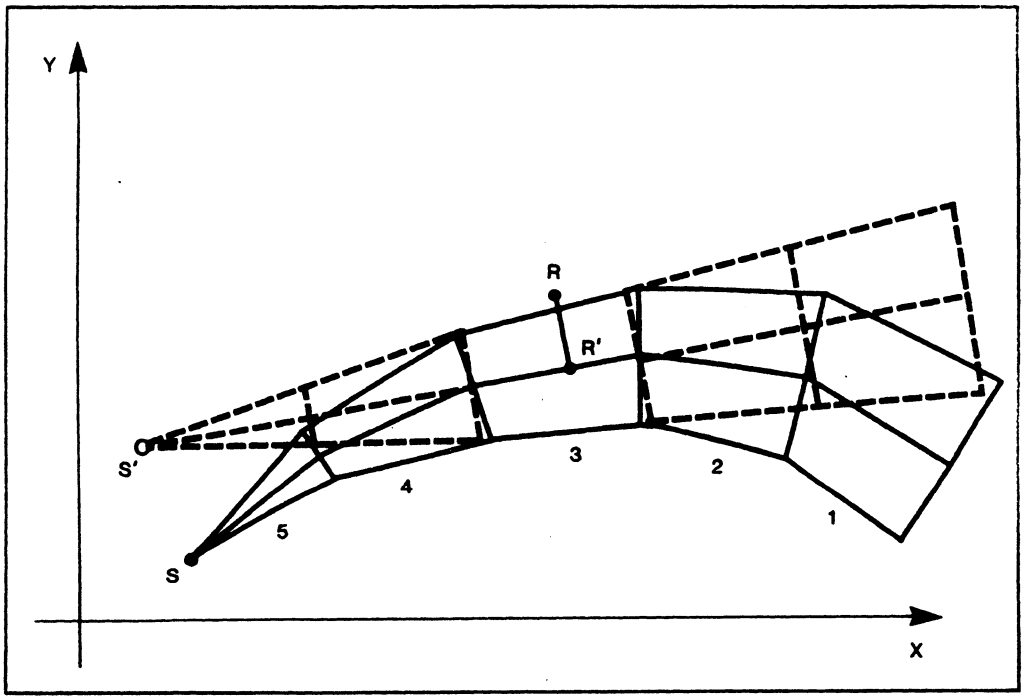

Figure 7-9. Computation of the concentration at the receptor R generated by the segmented plume (solid lines). The computation is performed by evaluating the contribution of the virtual plume (dotted lines) from the virtual source S' passing through the closest segment (number 3) to the receptor R (from Zannetti, 1986). [Reprinted with permission from Pergamon Press.]

still basically computed by Equation 7–1 and that represents the contribution of the entire virtual plume passing through that segment, as Figure 7–9 illustrates. Therefore, only one segment (the closest) affects the concentration computation at each receptor, except that the occurrence of a 180° wind direction change can create a condition where the contribution of two segments (that is, two virtual plumes) should be superimposed at some receptors.

7.8 PUFF MODELS

Puff models (e.g., Lamb, 1969; Roberts et al., 1970) have, like segmented models, been developed to treat nonstationary emissions in nonhomogeneous dispersion conditions. Puff methods, however, have the additional advantage of being able, at least theoretically, to simulate calm or low wind conditions.

The Gaussian puff model assumes that each pollutant emission of duration Δt injects into the atmosphere a mass $\Delta M = Q\Delta t$, where Q is the time-varying emission rate. The center of the puff containing the mass ΔM is advected according to the local time-varying wind vector. If, at time t, the center of a puff is located at $\mathbf{p}(t) = (x_p, y_p, z_p)$, then the concentration due to that puff at the receptor $\mathbf{r} = (x_r, y_r, z_r)$ can be computed using the basic Gaussian puff formula

$$\Delta c = \frac{\Delta M}{(2\pi)^{3/2}\,\sigma_h^2\,\sigma_z}\exp\left[-\frac{1}{2}\left(\frac{x_p - x_r}{\sigma_h}\right)^2\right]\exp\left[-\frac{1}{2}\left(\frac{y_p - y_r}{\sigma_h}\right)^2\right] \cdot \exp\left[-\frac{1}{2}\left(\frac{z_p - z_r}{\sigma_z}\right)^2\right] \tag{7–46}$$

which is often expanded to incorporate reflection and deposition/decay terms. Note that the analytical integration of Equation 7–46 in stationary, homogeneous transport conditions gives the Gaussian plume formula of Equation 7–4.

Equation 7–46 requires the proper evaluation of the horizontal (σ_h) and vertical (σ_z) dynamics of each puff's growth. The total concentration in a receptor at time t is computed by adding the contribution Δc from all existing puffs generated by all sources. Note that the "puff" Equation 7–46 differs from the "plume" Equation 7–4 mainly because an extra horizontal diffusion term has been substituted for the transport term, with the consequent disappearance of the wind speed $\bar{u}$. In other words, in a puff model, the wind speed affects the concentration computation only by controlling the density of puffs in the region (that

is, the lower the wind speed, the closer a puff is to the next one generated by the same source). Therefore, at least in theory, a puff model can handle calm or low-wind conditions, and this approach represents the most advanced and powerful application of the Gaussian formula.

Several studies have discussed the puff modeling approach in detail, improving its application features. In particular, algorithms were proposed and evaluated for incorporating wind shear effects (Sheih, 1978); virtual distance (Ludwig et al., 1977) and virtual age (Zannetti, 1981) computations were defined for correctly evaluating the σ_h and σ_z dynamics of the puff; puff merging (Ludwig et al., 1977) or puff splitting (Zannetti, 1981) were incorporated for performing cost-effective simulations with relatively large Δt (for example, 5 to 10 minutes); and an empirical method was derived (Zannetti, 1981) for evaluating the puff's σ_h and growth during calm or low-wind conditions as a function of currently available σ functions during transport conditions.

The determination of the puff modeling sigmas can be confusing, as discussed by Hanna et al. (1982). There are, in fact, two types of application for puff modeling. The one discussed above uses puffs to simulate the average characteristics (e.g., one-hour average concentrations) of a continuously emitted plume. In this case, it is correct to use the plume sigmas discussed in Section 7.2 to describe the growth of each puff in the plume. But puff (or better, relative diffusion) simulations apply also to the instantaneous or semi-instantaneous sources, defined as those sources where the release time or the sampling time is short compared with the travel time.

Unfortunately, little information is available for the description of the diffusion of a single puff, i.e., for the evaluation of the relative diffusion sigmas, even though it is clear that the plume sigma equations described in Section 7.2 cannot be applied (even though they often are) to relative diffusion calculations.

For relative diffusion, Hanna et al. (1982) recommend the Batchelor's formula

$$\sigma_h^2 = \epsilon t^3 \qquad (7\text{-}47)$$

for puff travel times that are less than 10^4 s, where ϵ is the eddy dissipation rate. They also recommend calculating ϵ locally at first, and then at a height $z = z_i/2$ as σ_z approaches $0.3\ z_i$. The eddy dissipation rate ϵ is given by

$$\epsilon = \frac{u_*^3}{k\,z}\left(\phi_m - \frac{z}{L}\right) \tag{7-48}$$

in the surface layer (ϕ_m was discussed in Section 3.6), while, at heights above the surface layer at midday,

$$\epsilon \simeq 0.5\,H' \tag{7-49}$$

The term H' is the surface buoyancy flux

$$H' = \frac{g}{T}\,\overline{w'T'} = \frac{H\,g}{c_p\,\varrho\,T} \tag{7-50}$$

where H is the surface heat flux defined by Equation 3-21. In neutral conditions, however, $H' = 0$ and, consequently, $\epsilon = 0$. In this case, a better fit of the available data gives, above the surface layer

$$\epsilon = u_*^3/(0.5\,z) \tag{7-51}$$

For travel times greater than 10^4 s, Hanna et al. (1982) suggest

$$\sigma_h = const\ t \tag{7-52}$$

where *const* can be determined by forcing Equation 7-52 to satisfy Equation 7-47 for $t = 10^4$ s, thus giving

$$const = 100\sqrt{\epsilon} \tag{7-53}$$

A similar procedure is proposed for σ_z, except that σ_z is recommended to remain equal to $0.3\ z_i$ for all times after it first reaches this value.

7.9 MIXED SEGMENT-PUFF METHODOLOGY

Zannetti (1986) has recently proposed a new mixed methodology that combines the advantages of both the segment and puff approaches for realistic

and cost-effective simulation of short-term plume dispersion phenomena using the Gaussian formula.

Pollutant dynamics are described by the temporal evolution of plume elements, treated as segments or puffs according to their size. While the segments provide a numerically fast simulation during transport conditions, the puffs allow a proper simulation of calm or low-wind situations.

The methodology is incorporated into a computer package (AVACTA II, Release 3) that gives the user large flexibility in defining the computational domain, the three-dimensional meteorological and emission input, the receptor locations, and in selecting plume rise and sigma fomulae. AVACTA II provides both pollutant concentration fields and dry/wet deposition patterns. The model uses linear chemistry and is applicable to any two-species reaction chain (e.g., SO_2 and SO_4^{2-}), where this approximation is reasonable and an appropriate reaction rate is available.

According to this dynamic segment-puff approach, each plume is described by a series of elements (segments or puffs) whose characteristics are updated at each dispersion time interval Δt (for example, 5 to 10 minutes). Meteorological three-dimensional fields (wind and turbulence status) and emission parameters are allowed to change at each "meteorological" time step Δt_m (typically, 30 to 60 minutes). The dynamics of each element consist of (1) generation at the source; (2) plume rise; (3) transport by advective wind; (4) diffusion by atmospheric turbulence; (5) ground deposition, dry and wet; and (6) chemical transformation, creating secondary pollutant from a fraction of the primary pollutant. The type of element (segment or puff) does not affect its dynamics, but only the computation of the concentration field, which is discussed in Section 7.9.6.

Each element is characterized by the following time-varying parameters (see the example in Figure 7-10) evaluated at its final central point B:

$\mathbf{e} = (x_e, y_e, z_e)$	coordinates of the point B
h_e	elevation of B above the ground (in flat terrain $h_e = z_e$)
M_1, M_2	masses of primary and secondary pollutant
$\sigma_h, \sigma_{z1}, \sigma_{z2}$	standard deviations of the Gaussian concentration distribution; horizontal, vertical below B, and vertical above B, respectively

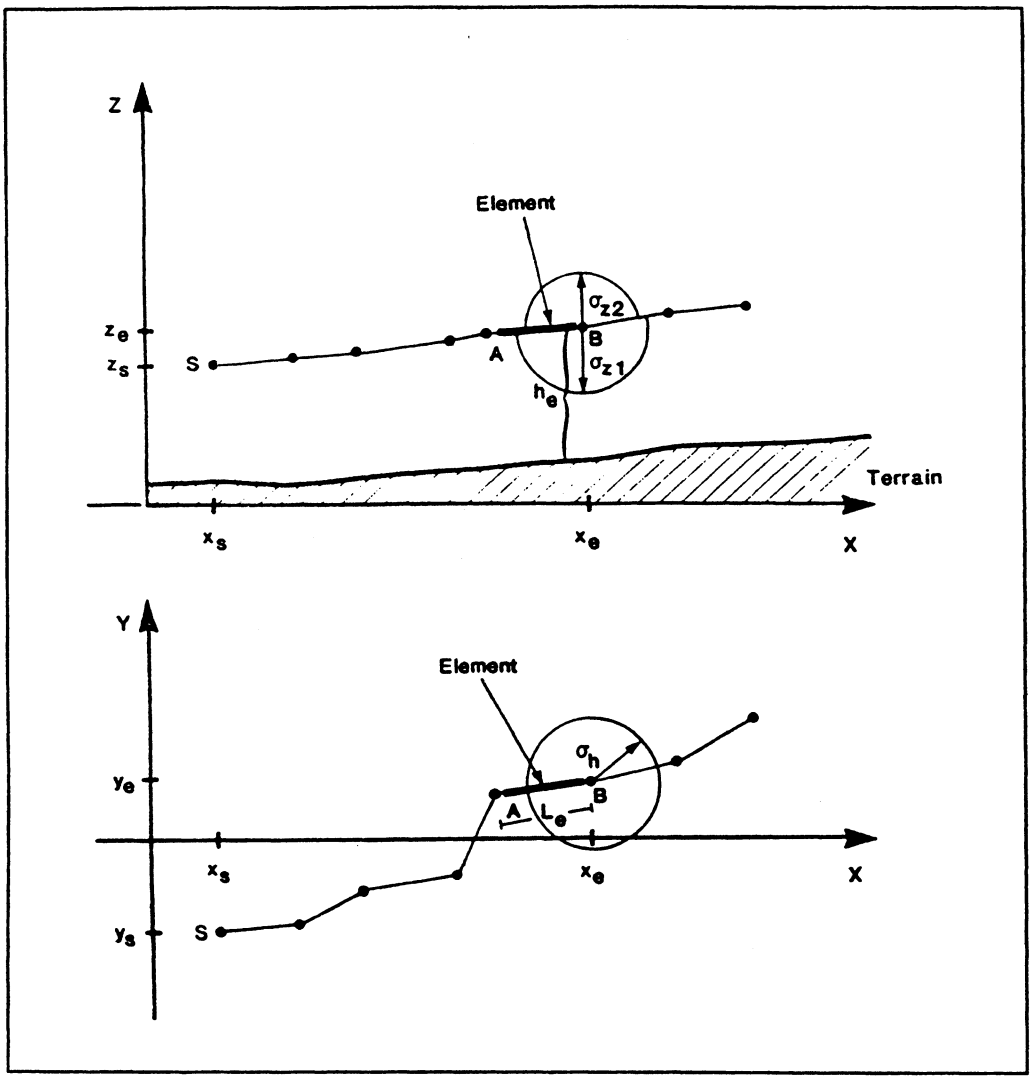

Figure 7–10. Chain of elements from the source S at time t. The time–varying parameters of a selected element in the chain are illustrated (from Zannetti, 1986). [Reprinted with permission from Pergamon Press.]

The characteristics of each element's initial central point A at time t are equal to those, at the same time t, of the final central point of the element successively emitted from the same source.

7.9.1 Generation of Plume Elements

At each time interval Δt, a new element is added to the element "chain" from each source. The parameters defining each new element have the following

initial values: the central final point is set at the source's exit point plus the vertical plume rise Δh; $M_1 = Q_1 \Delta t$, $M_2 = Q_2 \Delta t$, where Q_1 and Q_2 are the current emission rates of primary and secondary pollutants (generally $Q_2 = 0$); and σ_h, σ_{z1}, and σ_{z2} represent the initial sigmas of the plume (for example, 0.369 multiplied by the source exit diameter may be chosen for σ_h, and $\Delta h/3.16$ for σ_{z1} and σ_{z2}).

7.9.2 Transport

At each time interval Δt, the central final point of each existing element is advected according to the current wind vector $\bar{\mathbf{u}} = (u_x, u_y, u_z)$ averaged over the volume covered by the element size (i.e., $\pm 2\sigma$), as follows

$$\mathbf{e}^{(new)} = \mathbf{e}^{(old)} + \bar{\mathbf{u}} \Delta t \tag{7-54}$$

However, if the horizontal transport term

$$u_h = (u_x^2 + u_y^2)^{1/2} \tag{7-55}$$

is less than a critical value $u_{\min}$ (for example, $u_{\min} = 1$ m s^{-1}), u_x and u_y are forced to zero, since it is assumed that such small terms represent more local intermittent effects than actual transport. In this case, however, a large horizontal diffusion may be produced by the large wind direction fluctuations typically encountered during these low wind speed situations.

7.9.3 Diffusion

During each Δt, the element's sigmas are increased based on the virtual distance/age concept (Ludwig et al., 1977; Zannetti, 1981), which operates for either σ_h, σ_{z1}, or σ_{z2}, according to the following scheme.

1. Select the current sigma function $\sigma = \sigma(d)$ for the element (d is the downwind distance) according to the current local meteorology at the element's location; that is, the average atmospheric turbulent status in the volume covered by the element size (atmospheric turbulence status is often represented simply by a "stability class," a discrete number).

2. Evaluate the virtual distance d_v such as

$$\sigma^{(old)} = \sigma(d_v) \tag{7-56}$$

where $\sigma^{(old)}$ is the current sigma value for the element. The computation in Equation 7–56 is straightforward for some sigma formulae (for example, power laws), but requires iterative procedures for others.

3. If $u_h < u_{\min}$ force $u_h = u_{\min}$.

4. Increment sigma by

$$\sigma^{(new)} = \sigma(d_v + u_h \Delta t) \tag{7-57}$$

The above dynamics of the element's sigmas depend upon the choice of the sigma function and the current atmospheric turbulence status at the element's location. A separate turbulence status can be considered for the computation of horizontal (σ_h) and vertical (σ_{z1}, σ_{z2}) increments, if a proper meteorological input is available. For example, the vertical temperature gradient might provide an evaluation of the "vertical" turbulence status, while the horizontal wind direction fluctuation intensity provides a good estimate of the "horizontal" turbulence status. (Without the measurement of the horizontal wind direction fluctuation, the estimate of "horizontal" turbulence status may be quite wrong.) Different values of the vertical turbulence status above and below the element center generate different dynamics for σ_{z1} and σ_{z2}.

7.9.4 Dry and Wet Deposition

Both dry and wet deposition for the primary and secondary pollutants are simulated by first-order reaction schemes and are computed during each Δt by an exponential reduction of the pollutant mass

$$M_i^{(new)} = M_i^{(old)} \exp\left[-P_{i,j}\,\Delta t/360,000\right] \tag{7-58}$$

where i indicates the primary ($i = 1$) or the secondary ($i = 2$) pollutant, j indicates dry ($j = 1$) or wet ($j = 2$) deposition, and $P_{i,j}$ is the corresponding percentage of reduction per hour (% h^{-1}). All mass differences $M_i^{(old)} - M_i^{(new)}$ are deposited and accumulated on the ground.

If the two $P_{i,1}$ for dry deposition are not directly specified as input values, they can be obtained from the deposition velocity values as

$$P_{i,1} = 360,000\ V_i/\Delta z_e \tag{7-59}$$

where V_i are the current deposition velocities at the element's location, and $\Delta z_e = (2\sigma_{z1} + 2\sigma_{z2})$ is the vertical thickness of the element. Equation 7-59 applies only when the plume has reached the ground (that is, $2\sigma_{z1} \geq h_c$), otherwise $P_{i,1} = 0$.

If the two $P_{i,2}$ for wet deposition are not directly specified as input values, they can be obtained (Draxler and Heffter, 1981) from precipitation data as

$$P_{i,2} = S_i\ P_r/(10T_p) \tag{7-60}$$

where S_i are the pollutant scavenging ratios, P_r is the current average precipitation rate at the element's location (mm h^{-1}), and T_p is the thickness (m) of the precipitation layer.

7.9.5 Chemical Transformation

During each Δt, a first-order chemical reaction scheme is adopted, in which the chemical transformation term reduces the mass M_1 of primary pollutant and increases the mass M_2 of secondary pollutant in each element according to

$$M_1^{(new)} = M_1^{(old)} \exp\ (-k\ \Delta t/360,000) \tag{7-61}$$

$$M_2^{(new)} = M_2^{(old)} + (w_2/w_1)\ M_1^{(old)}\ [1 - \exp\ (-k\ \Delta t/360,000)] \tag{7-62}$$

where k is the current chemical transformation factor at the element location expressed as a percentage of reduction per hour (% h^{-1}), and w_i are the pollutant molecular weights ($i = 1, 2$).

7.9.6 Concentration Computation

The plume element dynamics can be computed independently from the type of element (segment or puff). The element type, however, is a key factor in computing the plume concentration field during each Δt. The criterion for

identifying the type of element is the ratio between its length L_e (the horizontal distance between A and B in Figure 7–10) and σ_h. For a segment

$$L_e/\sigma_h > 2 \tag{7–63}$$

and, for a puff,

$$L_e/\sigma_h \leq 2 \tag{7–64}$$

where the center of the puff is located in the middle between A and B. Since σ_h continues to grow with time, all segments will eventually become puffs.

The above algorithm assures that, when segments are transformed into puffs, the distance between two consecutive puffs will not be greater than $2\sigma_h$, which is the condition required (Ludwig et al., 1977) for a series of puffs to provide an almost perfect representation of a continuous plume. In calm or low wind speed conditions, $L_e = 0$ and the elements are generated as puffs directly from the source.

The above scheme allows a realistic and computationally efficient representation of calm, transport and transitional cases. For example, puffs can accumulate for a few hours in the region near the source during calm conditions, and subsequently be advected downwind when the stagnation breaks up. The concentration at each receptor point due to a certain source must account for the contribution of all elements generated from that source; specifically, the sum of the contributions of all existing puffs plus the contribution of the closest segment. This allows a proper dynamic representation of both calm and transport conditions, including the previously mentioned situation in which, due to a 180° change in wind direction, two sections of the same plume may affect the same receptor. In this latter case, in fact, we can generally assume that the elements of the oldest section of the plume may have already become puffs, thus allowing both sections of the plume to contribute to the concentration computation at that receptor.

7.9.6.1 Puff Contribution

The concentration contribution of a single puff at a receptor during each Δt is computed by Equation 7–46, which allows the computation of the primary pollutant concentration c_1 (or the secondary one c_2) from the current values of the puff's variables M_1 (or M_2), σ_h, and σ_{z1} (or σ_{z2} if the receptor is above the center of the puff). These variables are evaluated by interpolation at the center of the puff, that is, the point between its initial and final central points.

7.9.6.2 Segment Contribution

Because of the condition defined in Equation 7–63, each segment has sufficient length L_e to assure that the horizontal "stream-wise" diffusion (that is, diffusion along the length of the segment) can be neglected in comparison with the transport term. This is one of the basic assumptions for Equation 7–4, which is used as the numerical algorithm for computing the concentration field due to a plume segment. This computation requires the identification of the segment closest to the receptor and the use of the segment's variables for computing, with Equation 7–4, the concentration field generated by an equivalent plume passing through the segment, as illustrated in Figure 7–9. The parameters in Equation 7–4 are evaluated in the following way:

1. The segment's variables (M_1, M_2, σ_h, σ_{z1}, σ_{z2}) are interpolated at the point R′ (see Figure 7–9), the closest point to R along the segment centerline.

2. Q is evaluated as a "virtual" current emission rate; i.e.,

$$Q = \left(\frac{M_1}{\Delta t}\right) or \left(\frac{M_2}{\Delta t}\right) \tag{7–65}$$

3. $\bar{u}$ is evaluated as a "virtual" current wind speed; i.e.,

$$\bar{u} = \frac{L_e}{\Delta t} \tag{7–66}$$

(However, $\bar{u}$ is forced to be $\geq u_{\min}$ to avoid unrealistic "convergence" effects.)

4. σ_{z2} is used instead of σ_{z1}, if the receptor R is above the point R'.

Naturally, only the closest segment is used, since its contribution is a surrogate for that of the entire segmented portion of the plume.

7.9.6.3 The Treatment of the Segment–Puff Transition

The concentration computation described in the previous section allows the incorporation of all the advantages of both the puff and the segmented approach. Numerical problems, however, arise when the receptor is close to the point in the plume at which segments grow into puffs (see Zannetti, 1986, for a discussion of how these problems have been eliminated).

7.9.6.4 Splitting of Elements

The breaking of a plume into elements allows the evaluation of their dynamics as a function of the local time-varying meteorological conditions. In particular, during each Δt, the final central point of each element moves from an old to a new position. The horizontal component of this advective displacement is

$$\Delta \mathbf{d}_h = \mathbf{u}_h \, \Delta t \tag{7-67}$$

where $\mathbf{u}_h = (u_x, u_y)$ is the current local horizontal wind vector.

Large values of $|\Delta \mathbf{d}_h|$, due to an increase in wind speed or associated to a change in wind direction, may affect the elements' ability to represent the continuous plume by reducing resolution. The splitting technique, which was originally proposed for puff modeling simulations (Zannetti, 1981), is here incorporated for both puffs and segments and is illustrated in Figure 7-11. This splitting generates, when required, enough fictitious elements along the element's trajectory during Δt to maintain sufficient resolution. The splitting of an element's trajectory is performed to compute its concentration contribution at receptor R when (1) the receptor R is affected by that element, and (2) for puffs, when $|\Delta \mathbf{d}_h| > \sigma_h$ and, for segments, when $|\Delta \mathbf{d}_t| > \sigma_h$, where $\Delta \mathbf{d}_t$ is the component of $\Delta \mathbf{d}_h$ which is perpendicular to the segment's centerline.

In this splitting computation, the masses M_1 and M_2 of the element are equally distributed among the split elements along the trajectory from the old position to the new one.

7.10 DERIVATIONS OF THE GAUSSIAN EQUATIONS

The Gaussian equations can be derived from both Eulerian and Lagrangian considerations and that is the reason Gaussian models are discussed here separately from Eulerian models (Chapter 6) and Lagrangian models (Chapter 8).

There are several ways to derive the steady-state Gaussian plume Equation 7-4. Four methods will be discussed briefly in this section.

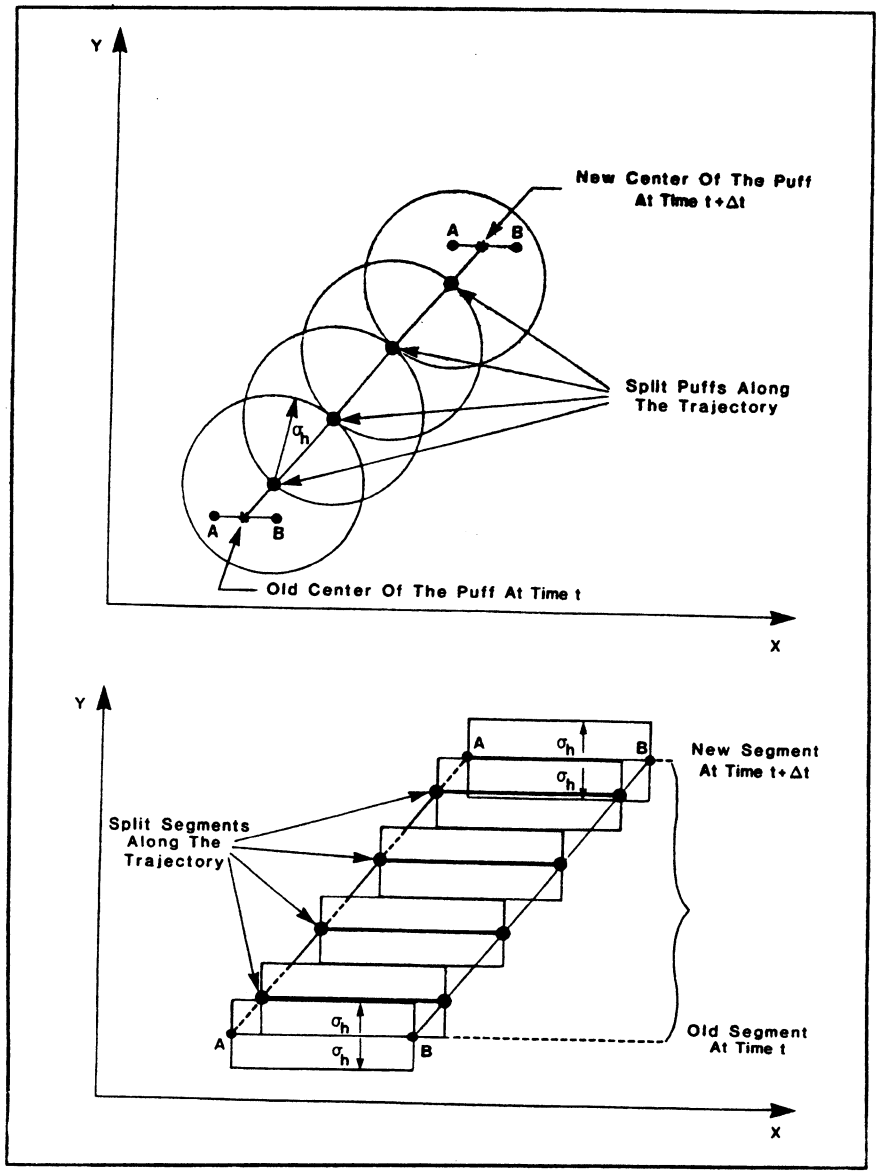

Figure 7–11. Splitting process for a puff (above) and a segment (below). A and B represent the initial and final central points of the element (from Zannetti, 1986). [Reprinted with permission from Pergamon Press.]

7.10.1 Semiempirical Derivation

The straightforward semiempirical derivation is performed by assuming that the plume concentration c, at each downwind distance x, has independent Gaussian distributions both in the horizontal and in the vertical. Therefore,

$$c(x,y,z) = const \frac{1}{\sqrt{2\pi}\sigma_h} \exp\left[-\frac{1}{2}\left(\frac{\Delta_{cw}}{\sigma_h}\right)^2\right] \cdot \frac{1}{\sqrt{2\pi}\sigma_z} \exp\left[-\frac{1}{2}\left(\frac{h_e - z_r}{\sigma_z}\right)^2\right] \tag{7-68}$$

where the symbols are the same as in Section 7.1 but x is used as the downwind distance instead of d.

The mass conservation condition requires all concentration fluxes through each plume cross-sectional plane (y,z) to be the same; i.e., for each x

$$Q = \int_{(y,z)} c(x,y,z)\,\bar{u}\,dydz \tag{7-69}$$

which, with Equation 7–68, gives $const = Q/\bar{u}$, and therefore Equation (7–4).

7.10.2 Gaussian Plume as Superimposition of Gaussian Puffs

A plume can be represented by an infinite series of infinitesimal puffs, where each puff, located in x,y,z, generates the concentration field

$$dc(x,y,z) = \frac{dM}{(2\pi)^{3/2}\sigma_x\sigma_y\sigma_z} \cdot \exp\left\{-\frac{1}{2}\left[\left(\frac{x-x_r}{\sigma_x}\right)^2 + \left(\frac{y-y_r}{\sigma_y}\right)^2 + \left(\frac{z-z_r}{\sigma_z}\right)^2\right]\right\} \tag{7-70}$$

at the receptor (x_r, y_r, z_r), and $dM = Q\,dt = Q\,dx/\bar{u}$ is the mass of the puff. Then, the integration along x of Equation 7–70 gives Equation 7–4, if $\sigma_x = \sigma_y = \sigma_h$.

7.10.3 Analytical Solution of the Steady-State Atmospheric Diffusion Equation 6–8

Several papers provided a derivation of Equation 7–4 by analytical integration of Equation 6–8 under certain simplifying homogeneous conditions

(e.g., Veigele and Head, 1978; Huang, 1979; Melli and Runca, 1979; Lupini and Tirabassi, 1979; Robson, 1983; Seinfeld, 1986). We should not state, however, that the Gaussian Equation 7–4 is a *particular* solution of Equation 6–8. In fact, if Equation 7–4 is derived from Equation 6–8, a condition is imposed on the plume's σ_h and σ_z. In the homogeneous case, this condition is

$$\sigma_h = \sqrt{2\,K_{11}\,x/\bar{u}} = \sqrt{2\,K_{22}\,x/\bar{u}} \tag{7–71}$$

and

$$\sigma_z = \sqrt{2\,K_{33}\,x/\bar{u}} \tag{7–72}$$

Equations 7–71 and 7–72 limit the sigma growth so that it is proportional to $x^{0.5}$, while Gaussian plume simulations benefit from the use of semiempirical σ functions that vary from $\sim x^{0.5}$ to $\sim x^{1.5}$.

Numerical and analytical integrations of Equation 6–8 in *nonhomogeneous* conditions show concentration solutions that are more realistic, in the sense that the plume sigmas are proportional to x^b with $b > 0.5$. Nevertheless, K–theory simulations always present difficulties in reproducing dispersion experiments in unstable conditions. What we want to emphasize here, however, is that the Gaussian equation cannot be considered a particular solution of Equation 6–8, even though its *form* can.

7.10.4 The Gaussian Equations as a Particular Solution of the Lagrangian Equation

All Gaussian plume and puff equations can be seen as a particular solution of the fundamental Lagrangian Equation 8–1, as discussed in the next Chapter.

REFERENCES

Benkley, C.W., and A. Bass (1979): Development of mesoscale air quality simulation models; Volume 3, User's Guide to MESOPUFF (Mesoscale Puff) model. EPA Document 600/7-79-XXX, Research Triangle Park, North Carolina. (See also Scire et al. (1984): User's guide to the MESOPUFF II model and related processor programs. EPA Document 600/8-84-013.)

Best, P.R., M. Kanowski, L. Stumer, and D. Green (1986): Convection dispersion modeling utilizing acoustic sounder information. *Atmos. Res.*, **20**:173.

Bowers, J., J. Bjorklund, and C. Cheney (1979): Industrial source complex (ISC) dispersion model user's guide, Vol. I. Research Triangle Park, North Carolina. EPA Document EPA-450/4-79-030. NTIS Publication PB80-133044.

Briggs, G.A. (1973): Diffusion estimation for small emissions, in environmental research laboratories. Air Resources Atmospheric Turbulence and Diffusion Laboratory 1973 Annual Report. USAEC Report ATDL-106, National Oceanic and Atmospheric Administration, December 1974.

Briggs, G.A. (1985): Analytical parameterization of diffusion: The convective boundary layer. *J.Climate and Appl. Meteor.*, **24**:1167.

Calder, K.L. (1971): *Proceedings,* 2nd Meeting of Expert Panel Air Pollution Modeling, NATO/CCMS Air Pollution, No. 5.

Chan, M.W., and I.H. Tombach (1978): AVACTA -- Air pollution model for complex terrain applications. AeroVironment Inc., Monrovia, California.

Chan, M.W. (1979): A tracer experiment to determine the transport and diffusion of an elevated plume in complex terrain. *Proceedings*, 72nd Annual APCA Meeting, Cincinnati, Ohio, June.

Chan, M.W., S.J. Head, and S. Machiraju (1979): Development and validation of an air pollution model for complex terrain application. Paper presented at NATO/CCMS Air Pollution Pilot Study. Rome, Italy. AeroVironment Technical Paper 9559, Monrovia, California.

DeMarrais, G.A. (1978): Atmospheric stability class determinations on a 481-meter tower in Oklahoma. *Atmos. Environ.*, **12**:1957-1964.

Dobbins, R.A. (1979): *Atmospheric Motion and Air Pollution*. John Wiley & Sons, New York.

Draxler, R.R. (1976): Determination of atmospheric diffusion parameters. *Atmos. Environ.*, **10**:99-105.

Draxler, R.R., and J.L. Heffler (1981): Workbook for estimating the climatology of regional-continental scale atmospheric dispersion and deposition over the United States. NOAA Technical Memorandum ERL ARL-96, Air Resources Laboratories, Silver Spring, Maryland.

Environmental Research and Technology, Inc. (1984): User's guide to the rough terrain diffusion model (RTDM). Environmental Research and Technology Document M2209-585, Concord, Massachusetts.

Fabrick, A., R.C. Sklarew, and J.D. Wilson (1977): *Point Source Modeling*. Form & Substance, Inc., Westlake Village, California.

Gifford, F.A. (1961): Use of routine meteorological observations for estimating the atmospheric dispersion. *Nucl. Safety*, **2**(4):47-57.

Gifford, F.A. (1976): Consequences of effluent release. *Nucl. Safety*, **17**(1):68-86.

Green, A.E., R.P. Singhal, and R. Venkateswar (1980): Analytic extensions of the Gaussian plume model. *JAPCA*, **30**(7):773–776.

Gryning, S.E., A.A. Holtslag, J.S. Irwin, and B. Sivertsen (1987): Applied dispersion modeling based on meteorological scaling parameters. *Atmos. Environ.*, **21**:79–89.

Hales, J.M., D.C. Powell, and T.D. Fox (1977): STRAM -- An air pollution model incorporating non-linear chemistry, variable trajectories, and plume segment diffusion. U.S. EPA Document 450/3-77-012, Research Triangle Park, North Carolina.

Hanna, S.R., et al. (1977): AMS Workshop on Stability Classification Schemes and Sigma Curves -- Summary of Recommendations. *J. Climate and Appl. Meteor.*, **58**(12):1305–1309.

Hanna, S.R., G.A. Briggs, and R.P. Hosker, Jr. (1982): Handbook on atmospheric diffusion. U.S. Department of Energy Document DOE/TIC-11223 (DE82002045), Office of Health and Environmental Research.

Hanna, S.R., L.L. Schulman, R.J. Paine, and J.E. Pleim (1984): Users guide to the offshore and coastal dispersion (OCD) model. Environmental Research and Technology, Concord, Massachusetts. Contract No. 14-08-0001-21138.

Hanna, S.R. (1989): Plume dispersion and concentration fluctuations in the atmosphere. Chapt. 14 *Encyclopedia of Environmental Control Techology*. Vol. 2. P.N. Cheremisinoff, editor. Houston, Texas: Gulf Publishing Company.

Harvey, Jr., R.B., and J.N. Hamawi (1986): A modification of the Gaussian dispersion equation to accommodate restricted lateral dispersion in deep river valleys. *APCA Note-Book*, **36**:171.

Huang, C.H. (1979):A theory of dispersion in turbulent shear flow. *Atmos. Environ.*, **13**:453.

Irwin, J.S. (1979): Estimating plume dispersion -- A recommended generalized scheme. Presented at 4th AMS Symposium on Turbulence and Diffusion, Reno, Nevada.

Irwin, J.S. (1980): Dispersion estimates suggestion #9: Processing of wind data. U.S. EPA Docket Reference No. II-B-33, Research Triangle Park, North Carolina.

Ludwig, F.L., L.S. Gasiorek, and R.E. Ruff (1977): Simplification of a Gaussian puff model for real-time minicomputer use. *Atmos. Environ.* **11**:431–436.

Lupini, R. and T. Tirabassi (1979): Gaussian plume model and advection-diffusion equation: An attempt to connect the two approaches. *Atmos. Environ.*, **13**:1169–1174.

Lyons, W.A., and H.S. Cole (1983): Fumigation and plume trapping on the shores of Lake Michigan during stable onshore flow. *J. Appl. Meteor.*, **12**:494–510.

Lamb, R.G. (1969): An air pollution model of Los Angeles. M.S. thesis, University of California, Los Angeles, 120 pp. (see Lamb, R.G., and M. Neiburger (1971): An interim version of a generalized urban diffusion model. *Atmos. Environ.*, **5**:239–264).

Martin, D.O. (1971): An urban diffusion model for estimating long-term average values of air quality. *JAPCA*, **21**:16–23.

McElroy, J.L., and F. Pooler (1968): St. Louis dispersion study; Volume II, Analysis. National Air Pollution Control Administration, Publication AP-53, 51. U.S. Dept. of Health, Education and Welfare, Arlington, Virginia.

Melli, P., and E. Runca (1979): Gaussian plume model parameters for ground-level and elevated sources derived from the atmospheric diffusion equation in a neutral case. *J. Appl. Meteor.*, **18**:1216–1221.

Pasquill, F. (1971): Atmospheric dispersion of pollution. *J. Roy. Meteor. Soc.*, 97:369–395.

Panofsky, H.A., and J.A. Dutton (1984): *Atmospheric Turbulence*. New York: John Wiley.

Pasquill, F. (1976): Atmospheric dispersion parameters in Gaussian plume modeling; Part 2, Possible requirements for change in the Turner Workbook values. U.S. EPA Document EPA–600/4–76–030b, Washington, D.C.

Phillips, P., and H.A. Panofsky (1982): A reexamination of lateral dispersion from continuous sources. *Atmos. Environ.*, *16*:1851–1859.

Roberts, J.J., E.S. Croke, and A.S. Kennedy (1970): An urban atmospheric dispersion model. *Proceedings*, Symposium on Multiple–Source Urban Diffusion Models. Air Pollution Control Office Publication AP–86, pp. 6.1–6.72.

Robson, R.E. (1983): On the theory of plume trapping by an elevated inversion. *Atmos. Environ.*, **17**:1923–2930.

Runca, E. (1977): Transport and diffusion of air pollutants from a point source. *Proceedings*, IFIP Working Conference on Modeling and Simulation of Land, Air and Water Resource System, Ghent, Belgium.

Schulman, L.L., and J.S. Scire (1980): Development of an air quality dispersion model for aluminum reduction plants. Environmental Research and Technology. Document P–7304A, Concord, Massachusetts.

Schulman, L.L., and S.R. Hanna (1986): Evaluation of downwash modification to the industrial source complex model. *JAPCA*, **36**:256–264.

Seinfeld, J.H. (1986): *Atmospheric Chemistry and Physics of Air Pollution*. New York: John Wiley & Sons.

Sheih, C.M. (1978): A puff pollutant dispersion model with wind shear and dynamic plume rise. *Atmos. Environ.*, **12**:1933–1938.

Smith, M.E. (1968): Recommended guide for the prediction of the dispersion of airborne effluents. 1st edition. American Society of Mechanical Engineers, New York.

Stern, A.C., Ed. (1976): *Air Pollution*. Volume I, 3rd Edition. New York: Academic Press.

Strimaitis, D.G., D.C. DiCristofaro, and T.F. Lavery (1986): The complex terrain dispersion model. EPA Document EPA–600–D–85/220, Atmospheric Sciences Research Laboratory, Research Triangle Park, North Carolina.

Turner, D.B. (1970): Workbook of atmospheric dispersion estimates. EPA, Research Triangle Park, North Carolina. U.S. EPA Ref. AP–26 (NTIS PB 191–482.)

U.S. Environmental Protection Agency (1978): Guideline on air quality models. EPA Document EPA–450/2–78–025. Research Triangle Park, North Carolina.

U.S. Environmental Protection Agency (1986): Guideline on air quality models (Revised). U.S. EPA Document EPA–450/2–78–027R. Research Triangle Park, North Carolina.

van Dop, H., R. Steenkist, and F.T. Nieuwstadt (1979): Revised estimates for continuous shoreline fumigation. *J. Appl. Meteor.*, **18**:133–137.

Veigele, W.J., and J.H. Head (1978): Derivation of the Gaussian plume model. *JAPCA*, **28**:1139–1141.

Williamson, S.J. (1973): *Fundamentals of Air Pollution*. Reading, Massachusetts: Addison–Wesley.

Yamartino, R.J. (1977): A new method for computing pollutant concentrations in the presence of limited vertical mixing. *APCA Note-Book*, **27**(5):467.

Zannetti, P. (1981): An improved puff algorithm for plume dispersion simulation. *J. Applied Meteor.*, **20**(10):1203–1211.

Zannetti, P., and N. Al-Madani (1983a): Numerical simulations of Lagrangian particle diffusion by Monte-Carlo techniques. VIth World Congress on Air Quality (IUAPPA), Paris, May.

Zannetti, P., and N. Al-Madani (1983b): Simulation of transformation, buoyancy and removal processes by Lagrangian particle methods. Fourteenth ITM Meeting on Air Pollution Modeling and Its Application. Copenhagen, Denmark, September.

Zannetti, P. (1986): A new mixed segment–puff approach for dispersion modeling. *Atmos. Environ.*, **20**:1121–1130.